Heterologous vaccination regimens with self-amplifying RNA and Adenoviral COVID vaccines induce superior immune responses than single dose vaccine regimens in mice

Alexandra J Spencer[1*], Paul F McKay[2], Sandra Belij-Rammerstorfer[1], Marta Ulaszewska[1], Cameron D Bissett[1], Kai Hu[2], Karnyart Samnuan[2], Daniel Wright[1], Hannah R Sharpe[1], Ciaran Gilbride[1], Adam Truby[1], Elizabeth R Allen[1], Sarah C Gilbert[1], Robin J Shattock[2], Teresa Lambe[1]

Affiliations:

[1]The Jenner Institute, Nuffield Department of Medicine, University of Oxford, United Kingdom

[2]Department of Infectious Disease, Imperial College London, United Kingdom

**Correspondence to:* Alexandra J Spencer*, The Jenner Institute, ORCRB, Roosevelt Drive, Oxford OX3 7DQ. Email: alex.spencer@ndm.ox.ac.uk.*

Short title: Superior immunity with heterologous vaccination regimens

Abstract

Several vaccines have demonstrated efficacy against SARS-CoV-2 mediated disease, yet there is limited data on the immune response induced by heterologous vaccination regimens using alternate vaccine modalities. Here, we present a detailed description of the immune response, in mice, following vaccination with a self-amplifying RNA (saRNA) vaccine and an adenoviral vectored vaccine (ChAdOx1 nCoV-19/AZD1222) against SARS-CoV-2. We demonstrate that antibody responses are higher in two dose heterologous vaccination regimens than single dose regimens, with high titre neutralising antibodies induced. Importantly, the cellular immune response after a heterologous regimen is dominated by cytotoxic T cells and $Th1^{+}$ CD4 T cells which is superior to the response induced in homologous vaccination regimens in mice.

Introduction

A number of vaccines against SARS-CoV-2 have reached late-stage clinical trials with encouraging efficacy readouts and mass vaccination schemes already initiated across several countries. Multiple vaccine technologies are being advanced [1], but there is limited information on how these vaccine modalities may work in combination. With ongoing clinical trial assessment of numerous SARS-CoV-2 vaccines and new mass vaccination incentives, there is a recognised real-world scenario where individuals may be vaccinated with different vaccine modalities. However, the utility of vaccination regimens combining different types of vaccine approaches remains to be determined.

Self-amplifying RNA (saRNA) typically encodes the alphaviral replicase and a target antigen. Upon entry into the cytoplasm, the RNA is amplified with subsequent translation of the target antigen [2]. The SARS-CoV-2 saRNA vaccine has been demonstrated to be highly

47 immunogenic in preclinical animal models [3] and is progressing through clinical trial
48 assessment with promising results. Adenoviruses are a frequently used viral vector vaccine
49 technology, they can be rapidly made to GMP at large scale, and a single vaccination can be
50 sufficient to provide rapid immunity in individuals [4]. In particular, chimpanzee derived
51 adenoviruses (ChAd) have good safety profiles, whilst inducing strong cellular and humoral
52 immune response against multiple target disease antigens [5-7]. Previous studies have
53 demonstrated efficacy after vaccination with ChAdOx1 nCoV-19/AZD1222 against SARS-
54 CoV-2 mediated disease [8], with concomitant high titre humoral immune responses and a
55 measurable Th1-dominated cellular immune response [9,10]. Importantly, an immune profile
56 consistently observed across different animal species [11,12].
57
58 In this study, the immunogenicity of saRNA and ChAdOx1 vaccines expressing full-length
59 SARS-CoV-2 spike protein were assessed in mice following vaccination with different vaccine
60 modalities combination. We demonstrate robust antibody responses following
61 heterologous vaccination regimens, with high titre neutralising antibodies. The cellular
62 immune response is dominated by cytotoxic T cells secreting IFNγ and TNFα and antigen
63 specific CD4+ T cells of a Th1 phenotype, with significantly higher antigen specific responses
64 observed following heterologous vaccination than those responses induced in single vaccine
65 regimens.
66
67
68
69
70

71 **Results**

72 **Heterologous vaccination potentiates SARS-CoV-2 spike-specific antibody response**

73 It was previously shown that homologous prime-boost immunization with saRNA [3] or ChAd
74 [11] induced a SARS-CoV-2 spike-specific IgG response with neutralisation capacity. In this
75 series of experiments, we compared the immune response induced by heterologous,
76 homologous and single dose vaccination with ChAd and saRNA vaccine modalities.
77 Heterologous vaccination with either ChAd or saRNA prime and alternative boost (i.e. ChAd-
78 saRNA or saRNA-ChAd) or two doses of saRNA induced the highest IgG responses, compared
79 to mice vaccinated with a single dose of either ChAd or saRNA (Fig. 1A and Fig. S1A), with
80 strong correlation between the two independent IgG ELISA methods (Fig. S1B). This IgG
81 response showed mixed profile, with mainly IgG2 (IgG2a, IgG2b in both mouse strains and
82 IgG2c in CD1 mice) and IgG1 subclasses (in both mouse strains) (Fig. 2A and B), which was
83 similar to previously reported results after vaccination with ChAd alone (Silva-Cayetano in
84 press) or saRNA alone [3].
85 Comparable amounts of SARS-CoV-2 spike-specific IgM were detected in all vaccinated
86 groups (Fig. 1B), while heterologous vaccination with saRNA-ChAd induced higher serum
87 SARS-CoV-2 spike-specific IgA levels compared to single vaccination with either vaccine, in
88 both CD1 and BALB/c mice (Fig. 1B).
89 Two doses of vaccine were also shown to increase the avidity of the IgG towards SARS-CoV-
90 2 spike (Fig. 1C) compared to single administration of either vaccine, while antibody-
91 mediated neutralisation was measured across all groups of vaccinated mice, with
92 heterologous and two dose saRNA inducing significantly higher levels of neutralisation
93 compared to single dose vaccination regimens (Fig. 1D). Not surprisingly, a correlation was

94 measured between neutralisation and levels of IgG /IgA SARS-CoV-2 spike-specific
95 antibodies (Fig. S1C).
96 Flow cytometry staining enabled identification of SARS-CoV-2 spike-specific B cells in the
97 spleen of mice. The data demonstrated that all vaccination regimens induced a similar
98 number of antigen specific B cells (Fig. S2B), with similar numbers of germinal centre (GC)
99 and isotype class switched B cells observed in all groups of vaccinated mice.
100
101 **Heterologous vaccination induces strong Th1 type response**
102 Cell mediated immunity was also investigated following heterologous or homologous
103 ChAdOx1 and saRNA vaccination regimens. The highest IFNγ response detected by ELISpot
104 was observed in mice that received a heterologous combination of vaccines, this increase
105 was only statistically significant when compared to single administration of saRNA in both
106 strains of mice (Fig. 3A and B), or saRNA-ChAd compared to ChAd in BALB/c mice (Fig. 3B). In
107 agreement with earlier reports, ELISpot responses were primarily directed towards the S1
108 portion of the spike protein (Fig S3A), with a consistent breadth of response measured with
109 all vaccine combinations and in both strains of mice (Fig. 3A and B).
110 Phenotype and functional capacity of the T cell response was measured by intracellular
111 cytokine staining, together with memory T cell marker staining. Consistent with previously
112 published data, saRNA and ChAd vectors induced antigen specific $CD4^+$ T cells of a Th1 bias,
113 with minimal IL4 and IL10 production measured and a response dominated by production of
114 IFNγ and TNFα, regardless of the vaccination regimen (Fig. 4A). Antigen specific $CD4^+$ T cells
115 displayed mixed Teff and Tem phenotype, with no statistically significant differences
116 observed in the total number of cells (Fig. 4A) and cell subsets (Fig. S3C). As before, in mice
117 the cell-mediated response following vaccination was dominated by $CD8^+$ T cells, with much

118 higher levels of IFNγ and TNFα (in addition to upregulation of CD107a) seen in all vaccine
119 groups (Fig. 4B) compared to $CD4^+$ T cell responses. In addition, the highest frequency of
120 antigen specific cells, in both outbred and inbred strains of mice, was measured following
121 heterologous vaccination, regardless of vaccine order (Fig. 4B). Antigen specific $CD8^+$ T cells
122 displayed a predominantly Teff phenotype, with the highest number of total antigen specific
123 cells (Fig. 4B) observed in heterologous vaccinated animals.
124
125

126 **Discussion**

127 The current pandemic and extraordinary efforts to develop effective vaccines with
128 subsequent mass vaccination roll-out has highlighted the 'real-world' practicalities of global
129 vaccination campaigns. There are around 20 vaccines in Phase 3 clinical trial assessment,
130 and several vaccines have already reported efficacy with subsequent emergency licensure
131 granted in some countries. While each individual vaccine candidate has been thoroughly
132 tested for safety and efficacy, there have been no studies reported to date that have
133 examined the safety, efficacy or any added benefit of mixed modality vaccinations. Given
134 the real-world vaccination initiatives that are being progressed, there may be a scenario
135 wherein an individual receives a vaccine prime and a boost dose from different
136 manufacturers or of different vaccine types. This current pre-clinical study examined the
137 cellular and humoral immune responses in mice following vaccination with either the
138 ChAdOx adenoviral vector or the saRNA LNP in homologous or heterologous prime-boost
139 combinations and compared immunogenicity to single moiety vaccinations.

140

141 All prime-boost regimens elicited high levels of SARS-CoV-2 spike-specific antibodies with
142 neutralisation capacity and high avidity, levels that were greater than single vaccines alone.
143 While heterologous vaccination regimens induced the highest antibody responses post-
144 vaccination, homologous saRNA and ChAd induced higher antibody responses than single
145 dose regimens, consistent with previous data in mice, pigs and NHPs [11,12]. Importantly in
146 human clinical trials, strong enhancement of the antibody response was observed following
147 a booster dose of ChAdOx1[13] , with this regimen shown to provide efficacy against SARS-
148 CoV-2 disease in late-stage clinical trials[8]. The cell-mediated response was dominated by
149 cytotoxic T cells, with heterologous regimens inducing higher frequencies and total numbers

150 of antigen specific $CD8^+$ T cells. Although $CD4^+$ T cell responses were overall lower in
151 frequency and number than $CD8^+$ T cell responses, all vaccination regimens elicited $CD4^+$ T
152 cell responses of a Th1 type response, even in the Th2 biased BALB/c background, a
153 response indicating that the potential for antibody dependent enhancement (ADE) and
154 subsequent enhancement of respiratory disease (ERD) caused by Th2-type lung
155 immunopathology is reduced [14-16].
156
157 While there are no defined correlates of protection, Rhesus Macaques studies have
158 demonstrated a clear role for neutralising antibodies and also $CD8^+$ T cells [17]. In agreement,
159 human studies have demonstrated neutralising antibodies and T cells play an important role
160 in preventing severe disease and augmenting recovery from COVID-19[18]. Both vaccine
161 modalities elicited high numbers of antigen specific T cells, which were further increased in
162 the heterologous regimens. The majority of the IFNγ ELISpot response was directed against
163 the S1 spike protein, particularly the first half (317 AA) which does not include the RBD. Not
164 surprisingly two doses regimens induced higher antibody responses, with combination
165 regimens leading to simultaneous high levels of neutralising antibodies and T cell responses.
166
167 Vaccination regimens that induce a broad immune response (humoral and cell-mediated)
168 will likely be the best option for long-term protection against severe disease and will be best
169 placed if booster vaccinations are considered in the future. The logistical challenges of
170 administering vaccines in a rapidly evolving landscape of mass vaccination schemes, coupled
171 with limited global supply, underpins the need to generate data on mixing vaccine
172 modalities. The data described herein suggests clinical trials should progress to assess the

173 safety, immunogenicity and efficacy of heterologous vaccination regimens to help progress

174 global deployment and vaccine uptake against SARS-CoV-2.

175

176

177

178 **Methods**

179 **Ethics Statement;** Mice were used in accordance with the UK Animals (Scientific
180 Procedures) Act under project license number P9804B4F1 granted by the UK Home Office.
181 Age matched animals were purchased from commercial suppliers as a batch for each
182 experiment and randomly split into groups on arrival at our facility. Animals were group
183 housed in IVCs under SPF conditions, with constant temperature and humidity with lighting
184 on a 13:11 light-dark cycle (7am to 8pm). For induction of short-term anaesthesia, animals
185 were anaesthetised using vaporised IsoFlo®. All animals were humanely sacrificed at the end
186 of each experiment by an approved Schedule 1 method.

187

188 **Animals and Immunizations;** Outbred CD1Hsd:ICR (CD-1) (Envigo) (n=8 per group), Crl:CD1
189 (ICR) (Charles River) (n=8 per group) and inbred BALB/cOlaHsd (BALB/c) (Envigo) (n=6 per
190 group) mice of 7 weeks of age, were immunized intramuscularly (i.m.) in the musculus
191 tibialis with 10^8 infectious units (iu) of ChAdOx1 nCoV-19 [12] or 1µg saRNA [3]. Mice were
192 boosted i.m. with the relevant vaccine candidate 4 weeks later. All mice were sacrificed 3
193 weeks after the final vaccination with serum and spleens collected for analysis of humoral
194 and cell-mediated immunity.

195

196 **Pseudotype virus neutralisation assay;** A HIV-pseudotyped luciferase-reporter based
197 system was used to assess the neutralization ability of sera from vaccinated mice. In brief,
198 CoV S-pseudotyped viruses were produced by co- transfection of 293T/17 cells with a HIV-1
199 gag-pol plasmid (pCMV-Δ8.91, a kind gift from Prof. Julian Ma, St George's University of
200 London), a firefly luciferase reporter plasmid (pCSFLW, a kind gift from Prof. Julian Ma, St
201 George's University of London) and a plasmid encoding the S protein of interest (pSARS-

202 CoV2-S) at a ratio of 1:1.5:1. Virus- containing medium was clarified by centrifugation and
203 filtered through a 0.45 µm membrane 72 h after transfection, and subsequently aliquoted
204 and stored at −80 °C. For the neutralization assay, heat-inactivated sera were first serially
205 diluted and incubated with virus for 1 h, and then the serum-virus mixture was transferred
206 into wells pre-seeded Caco2 cells. After 48 h, cells were lysed, and luciferase activity was
207 measured using Bright-Glo Luciferase Assay System (Promega). The IC50 neutralization was
208 then calculated using GraphPad Prism (version 8.4). Statistical analyses were performed on
209 log transformed data.
210
211 **Antigen-specific IgG ELISA;** The antigen-specific IgG titres in mouse sera were assessed by a
212 semi-quantative ELISA. MaxiSorp high binding ELISA plates (Nunc) were coated with 100 µL
213 per well of 1 µg mL−1 recombinant SARS-CoV-2 protein with the pre-fusion stabilized
214 conformation in PBS. After overnight incubation at 4 °C, the plates were washed 4 times
215 with PBS-Tween 20 0.05% (v/v) and blocked for 1 h at 37 °C with 200 µL per well blocking
216 buffer (1% BSA (w/v) in PBS-Tween-20 0.05%(v/ v)). The plates were then washed and the
217 diluted samples or a 5-fold dilution series of the standard IgG added using 50 µL per well
218 volume. Plates were incubated for 1 h at 37 °C, then washed and secondary antibody added
219 at 1:2000 dilution in blocking buffer (100 µL per well) and incubated for 1 hr at 37 ^{o}C. After
220 incubation and washes, plates were developed using 50 µL per well SureBlue TMB (3,3', 5,5'-
221 tetramethylbenzidine) substrate and the reaction stopped after 5 min with 50 µL per well
222 stop solution (Insight Biotechnologies). The absorbance was read on a Versamax
223 Spectrophotometer at 450 nm (BioTek Industries). Statistical analyses were performed on
224 log-transformed data.
225

226 **Antigen specific Isotype ELISA;** MaxiSorp plates (Nunc) were coated with 50 µl of 2 µg/mL
227 or 50ul of 5 µg/mL ng/well SARS-CoV-2 FL-S protein overnight at 4 °C for detection of IgG
228 (250ng/well) or IgM and IgA (500ng/well), respectively, prior to washing in PBS/Tween
229 (0.05% v/v) and blocking with Blocker Casein in PBS (Thermo Fisher Scientific) for 1 h at
230 room temperature (RT). Standard positive serum (pool of mouse serum with high endpoint
231 titre against FL-S protein), individual mouse serum samples, negative and an internal control
232 (diluted in casein) were incubated for 2 hrs at room temperature for detection of specific
233 IgG or 1h at 37 ^{o}C for detection of specific IgM or IgA. Following washing, bound antibodies
234 were detected by addition of alkaline phosphatase (AP)-conjugated goat anti-mouse IgG
235 (Sigma-Aldrich) or anti-mouse IgM (Abcam) or anti-mouse IgA (SouthernBiotech) for 1h at
236 room temperature and addition of p-Nitrophenyl Phosphate, Disodium Salt substrate
237 (Sigma-Aldrich). An arbitrary number of ELISA units (EU) were assigned to the reference
238 pool and optical density values of each dilution were fitted to a 4-parameter logistic curve
239 using SOFTmax PRO software. ELISA units were calculated for each sample using the optical
240 density values of the sample and the parameters of the standard curve. IgM limit of
241 detection was defined a 2 ELISA Units, IgA limit of detection set as 6 ELISA Units. All data
242 was log-transformed for statistical analyses.
243
244 **Antigen Specific IgG Subclass ELISAs;** MaxiSorp plates (Nunc) were coated with 50 µL of 2
245 µg/mL per well of SARS-CoV-2 FL-S protein overnight at 4 °C prior to washing in PBS/Tween
246 (0.05% v/v) and blocking with Blocker Casein in PBS (Thermo Fisher Scientific) for 1 h at
247 room temperature (RT). For detection of IgG subclasses all serum samples were diluted to 1
248 total IgG EU and incubated at 37 ^{o}C for 1 h prior to detection with Alkaline Phosphatase
249 conjugated anti-mouse IgG subclass-specific secondary antibodies (Southern Biotech or

250 Abcam) incubated for 1 h at 37 ^{o}C . The results of the IgG subclass ELISA are presented using
251 optical density values.
252
253 **Avidity ELISA;** Anti-SARS-CoV-2 spike-specific total IgG antibody avidity was assessed by
254 sodium thiocyanate (NaSCN)-displacement ELISA. Nunc MaxiSorp ELISA plates (Thermo
255 Fisher Scientific) coated overnight at 4 °C with 2µg/well SARS-CoV-2 trimeric spike protein
256 diluted in PBS were washed with PBS/Tween (0.05% v/v) and blocked for 1 h with 100 µl per
257 well of Blocker Casein in PBS (Thermo Fisher Scientific) at 20 °C. Test samples and a positive
258 control serum pool were diluted in blocking buffer to 1 total IgG EU and incubated for 2 h at
259 20 °C. After washing, increasing concentrations of NaSCN (Sigma-Aldrich) diluted in PBS
260 were added and incubated for 15 min at 20 °C. Following another wash, bound antibodies
261 were detected by addition of AP-conjugated goat anti-mouse IgG (Sigma-Aldrich) for 1 h at
262 room temperature and addition of p-Nitrophenyl Phosphate, Disodium Salt substrate
263 (Sigma-Aldrich). For each sample, concentration of NaSCN required to reduce the OD405 to
264 50% of that without NaSCN (IC50) was interpolated from this function and reported as a
265 measure of avidity.
266
267 **Antigen specific B cell staining;** Spike, RBD and a decoy NANP$_9$C (repeat region from *P.*
268 *falciparum* CSP protein) tetramers were prepared in house by mixing biotinylated proteins
269 with streptavidin conjugated flurochromes (A488, A647 or r-PE) in a 4:1 molar ratio and
270 incubating on ice for 30 minutes. Splenocytes were stained with Spike-PE and RBD-A647 at a
271 final concentration of 0.04mM, whilst decoy tetramer, NANP$_9$C-A488 was used at a final
272 concentration of 0.4mM. Splenocytes were stained with Live-Dead Aqua and Fc block (anti-
273 CD16/32 mAb, Clone 93) prior to staining with the antibody cocktail containing NANP$_9$C-

274 Alexa488, GL7-PerCPCy5.5 (Clone GL7), CD138 BV421 (Clone 281-2), CD95-BV605 (Clone
275 SA367H8), CD4-BV650 (Clone GK1.5), CD279-BV711 (Clone 29F.1A12), CD19-BV780 (6D5),
276 RBD-A647, IgD-A700 (Clone 11-26c.2a), IgM-APCCy7 (Clone 11/41), Spike-PE, CD38-PECY5
277 (Clone 90), CD69 PeCy7 (Clone H1.2F3), CD45R-BUV395 (Clone RA3-6B2) and CD3-BUV496
278 (Clone 145-2C11), antibodies purchased from BioLegend, BD or Invitrogen. Antigen specific
279 B cells were identified by gating on LIVE/DEAD negative, doublet negative (FSC-H vs FSC-A),
280 size (FSC-H vs SSC), CD45RA^{+}, CD19^{+} and NANP-A488^{-}, RBD-A647^{+} and Spike-PE^{+}.
281
282 **ELISpot and ICS staining;** Spleen single cell suspension were prepared by passing cells
283 through 70µM cell strainers and ACK lysis prior to resuspension in complete media. For
284 analysis of IFNγ production by ELISpot, splenocytes were stimulated with two pools of S1
285 (pools 1 and 2) and two pools S2 (pools 3 and 4) peptides (final concentration of 2µg/mL) on
286 IPVH-membrane plates (Millipore) coated with 5µg/mL anti-mouse IFNγ (AN18). After 18-20
287 hours of stimulation at 37 ^{o}C, IFNγ spot forming cells (SFC) were detected by staining
288 membranes with anti-mouse IFNγ biotin (1mg/mL) (R46A2) followed by streptavidin-
289 Alkaline Phosphatase (1mg/mL) and development with AP conjugate substrate kit (BioRad,
290 UK).
291 For analysis of intracellular cytokine production, cells were stimulated at 37 ^{o}C for 6 hours
292 with 2µg/mL a pool of S1 (ELISpot pools 1 and 2) or S2 (ELISpot pools 3 and 4) peptides,
293 media or positive control cell stimulation cocktail (containing PMA-Ionomycin, BioLegend),
294 together with 1µg/mL Golgi-plug (BD) and 2µl/mL CD107a-Alexa647 (Clone 1D4B). Following
295 surface staining with CD3-A700 (Clone 17A2), CD4-BUV496 (Clone GK1.5), CD8-BUV496
296 (Clone 53-6.7), CD44-BV780 (Clone IM7), CD62L-BV711 (Clone MEL-14), CD69-PECy7 (Clone
297 H1.2F3) and CD127-BV650 (Clone A7R34) or CD127-APCCy7 (Clone A7R34), cells were fixed

298 with 4% paraformaldehyde and stained intracellularly with TNFa-A488 (Clone MP6-XT22),
299 IL2-PerCPCy5.5 (Clone JES6-5H4), IL4-BV605 (Clone 11B11), IL10-PE (Clone JES5-16E3) and
300 IFNγ-e450 (Clone XMG1.2) diluted in Perm-Wash buffer (BD). Sample acquisition was
301 performed on a Fortessa (BD) and data analyzed in FlowJo V10 (TreeStar). An acquisition
302 threshold was set at a minimum of 5000 events in the live $CD3^+$ gate. Antigen specific T cells
303 were identified by gating on LIVE/DEAD negative, doublet negative (FSC-H vs FSC-A), size
304 (FSC-H vs SSC), $CD3^+$, $CD4^+$ or $CD8^+$ cells and cytokine positive. Cytokine positive responses
305 are presented after subtraction of the background response detected in the corresponding
306 media stimulated control sample for each mouse and summing together the response
307 detected to each pool of peptides. T effector (Teff) cells were defined as $CD62L^-$ $CD127^-$, T
308 central memory cells defined as $CD62L^-$ $CD127^+$ and T central memory (Tcm) cells defined as
309 $CD62L^{hi}$ $CD127^{hi}$ (Figure S3B). All graphs and statistical analysis were performed using Prism
310 v9 (Graphpad), total cell counts were log transformed prior to statistical analysis.
311

312 **References**

313 1 Tregoning, J. S. *et al.* Vaccines for COVID-19. *Clin Exp Immunol* **202**, 162-192,
314 doi:10.1111/cei.13517 (2020).
315 2 Blakney, A. K. *et al.* Big Is Beautiful: Enhanced saRNA Delivery and Immunogenicity
316 by a Higher Molecular Weight, Bioreducible, Cationic Polymer. *ACS Nano* **14**, 5711-
317 5727, doi:10.1021/acsnano.0c00326 (2020).
318 3 McKay, P. F. *et al.* Self-amplifying RNA SARS-CoV-2 lipid nanoparticle vaccine
319 candidate induces high neutralizing antibody titers in mice. *Nature communications*
320 **11**, 3523, doi:10.1038/s41467-020-17409-9 (2020).
321 4 Ewer, K. *et al.* Chimpanzee adenoviral vectors as vaccines for outbreak pathogens.
322 *Hum Vaccin Immunother* **13**, 3020-3032, doi:10.1080/21645515.2017.1383575
323 (2017).
324 5 Antrobus, R. D. *et al.* Clinical assessment of a novel recombinant simian adenovirus
325 ChAdOx1 as a vectored vaccine expressing conserved Influenza A antigens. *Mol Ther*
326 **22**, 668-674, doi:10.1038/mt.2013.284 (2014).
327 6 Venkatraman, N. *et al.* Safety and Immunogenicity of a Heterologous Prime-Boost
328 Ebola Virus Vaccine Regimen in Healthy Adults in the United Kingdom and Senegal. *J*
329 *Infect Dis* **219**, 1187-1197, doi:10.1093/infdis/jiy639 (2019).

7 Folegatti, P. M. *et al.* Safety and immunogenicity of a candidate Middle East respiratory syndrome coronavirus viral-vectored vaccine: a dose-escalation, open-label, non-randomised, uncontrolled, phase 1 trial. *Lancet Infect Dis* **20**, 816-826, doi:10.1016/S1473-3099(20)30160-2 (2020).

8 Voysey, M. *et al.* Safety and efficacy of the ChAdOx1 nCoV-19 vaccine (AZD1222) against SARS-CoV-2: an interim analysis of four randomised controlled trials in Brazil, South Africa, and the UK. *Lancet* **397**, 99-111, doi:10.1016/S0140-6736(20)32661-1 (2021).

9 Ewer, K. J. *et al.* T cell and antibody responses induced by a single dose of ChAdOx1 nCoV-19 (AZD1222) vaccine in a phase 1/2 clinical trial. *Nat Med*, doi:10.1038/s41591-020-01194-5 (2020).

10 Barrett, J. R. *et al.* Phase 1/2 trial of SARS-CoV-2 vaccine ChAdOx1 nCoV-19 with a booster dose induces multifunctional antibody responses. *Nat Med*, doi:10.1038/s41591-020-01179-4 (2020).

11 Graham, S. P. *et al.* Evaluation of the immunogenicity of prime-boost vaccination with the replication-deficient viral vectored COVID-19 vaccine candidate ChAdOx1 nCoV-19. *NPJ Vaccines* **5**, 69, doi:10.1038/s41541-020-00221-3 (2020).

12 van Doremalen, N. *et al.* ChAdOx1 nCoV-19 vaccine prevents SARS-CoV-2 pneumonia in rhesus macaques. *Nature* **586**, 578-582, doi:10.1038/s41586-020-2608-y (2020).

13 Ramasamy, M. N. *et al.* Safety and immunogenicity of ChAdOx1 nCoV-19 vaccine administered in a prime-boost regimen in young and old adults (COV002): a single-blind, randomised, controlled, phase 2/3 trial. *Lancet* **396**, 1979-1993, doi:10.1016/S0140-6736(20)32466-1 (2021).

14 Wang, S. F. *et al.* Antibody-dependent SARS coronavirus infection is mediated by antibodies against spike proteins. *Biochem Biophys Res Commun* **451**, 208-214, doi:10.1016/j.bbrc.2014.07.090 (2014).

15 Tseng, C. T. *et al.* Immunization with SARS coronavirus vaccines leads to pulmonary immunopathology on challenge with the SARS virus. *PLoS One* **7**, e35421, doi:10.1371/journal.pone.0035421 (2012).

16 Lee, W. S., Wheatley, A. K., Kent, S. J. & DeKosky, B. J. Antibody-dependent enhancement and SARS-CoV-2 vaccines and therapies. *Nat Microbiol* **5**, 1185-1191, doi:10.1038/s41564-020-00789-5 (2020).

17 Mercado, N. B. *et al.* Single-shot Ad26 vaccine protects against SARS-CoV-2 in rhesus macaques. *Nature* **586**, 583-588, doi:10.1038/s41586-020-2607-z (2020).

18 Rydyznski Moderbacher, C. *et al.* Antigen-Specific Adaptive Immunity to SARS-CoV-2 in Acute COVID-19 and Associations with Age and Disease Severity. *Cell* **183**, 996-1012 e1019, doi:10.1016/j.cell.2020.09.038 (2020).

Acknowledgments: The authors would like to thank D. Pulido for provision of spike and RBD proteins, BMS staff for animal husbandry and management and A. Worth, J.Furze, M. Mykhaylyk and R. Evans for facilities support.

Funding: This report is independent research funded by the National Institute for Health Research (UKRI Grant Ref: MC_PC_19055, NIHR Ref: COV19 OxfordVacc-01). The views expressed in this publication are those of the author(s) and not necessarily those of the National Institute for Health Research or the Department of Health and Social Care.

Author Contributions: AJS, MU, SB-J, CB, KS, KM & PMK performed experiments. AJS, MU, HS, CG, EA & AT performed animal procedures and/or sample processing. AJS, SBJ, KH & PMK, analyzed data. AJS, TL, PMK, RS & SG designed the study. AJS, SBJ, TB wrote the manuscript. All authors reviewed the final version of the manuscript.

Competing interests: SCG is co-founder and board member of Vaccitech (collaborators in the early development of this vaccine candidate) and named as an inventor on a patent covering use of ChAdOx1-vectored vaccines and a patent application covering this SARS-CoV-2 vaccine. TL is named as an inventor on a patent application covering this SARS-CoV-2 vaccine and was consultant to Vaccitech. PMK and RJS are co-founders and RJS is a board member of VaxEquity and VacEquity and are named inventors on a patent application covering the SARS-CoV-2 saRNA vaccine candidate.

Figure legends

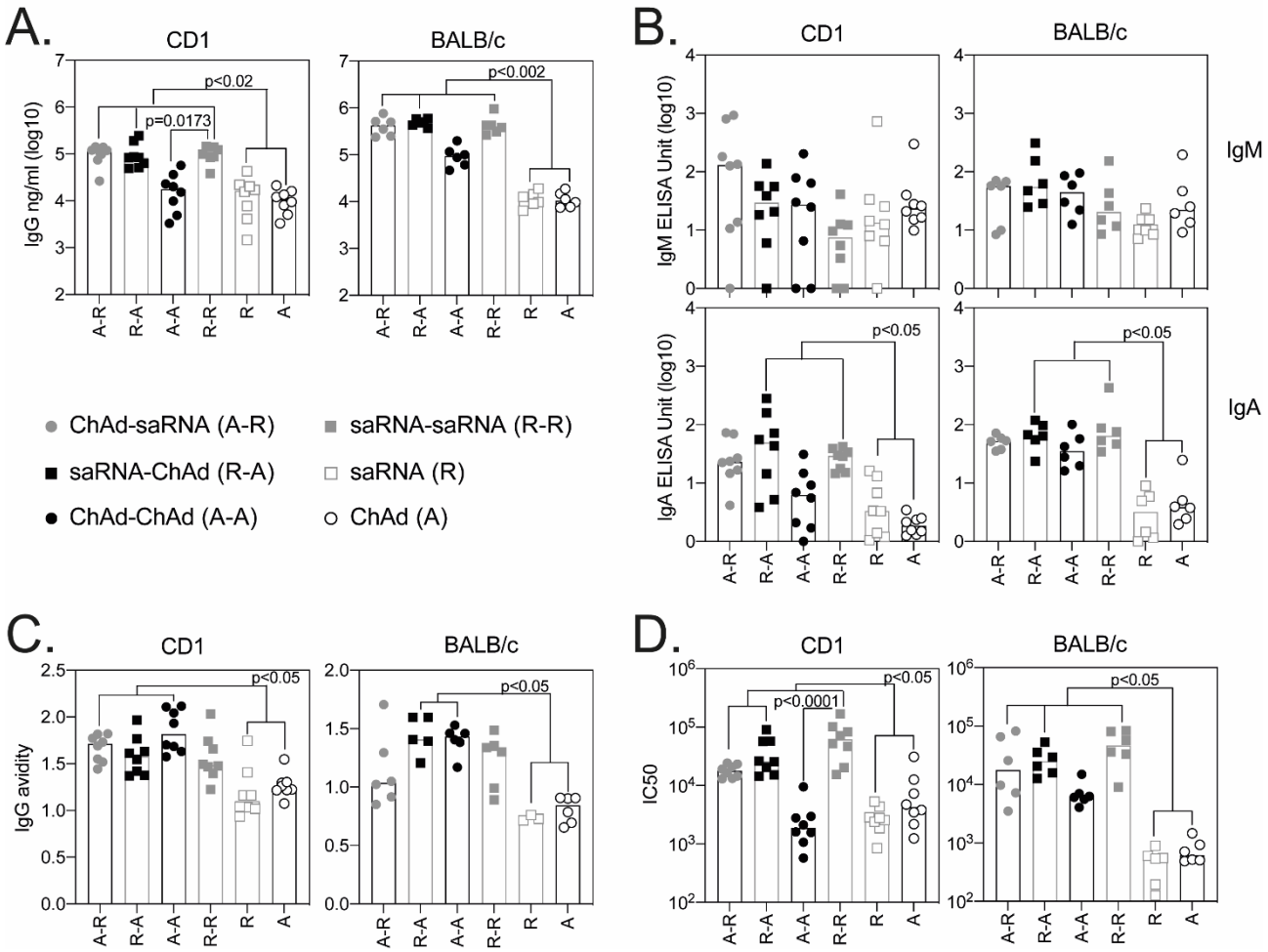

Fig 1: Antibody responses following ChAd and saRNA vaccination

Antibody responses were measured in the serum of mice collected 3 weeks after the final immunisation. Graphs show SARS CoV-2 spike-specific IgG (**A.**), IgM and IgA (**B.**) and IgG avidity (**C.**) measured by ELISA, and SARS-CoV-2 pseudotyped virus neutralisation (IC50) (**D.**). Individual mice are represented by a single data point, bars represent the median response in each group (CD1 n=8; BALB/c n=6). Data in each graph was analysed with a Kruskal-Wallis and post-hoc positive test to compare differences between vaccination groups, p values indicate significant differences between groups.

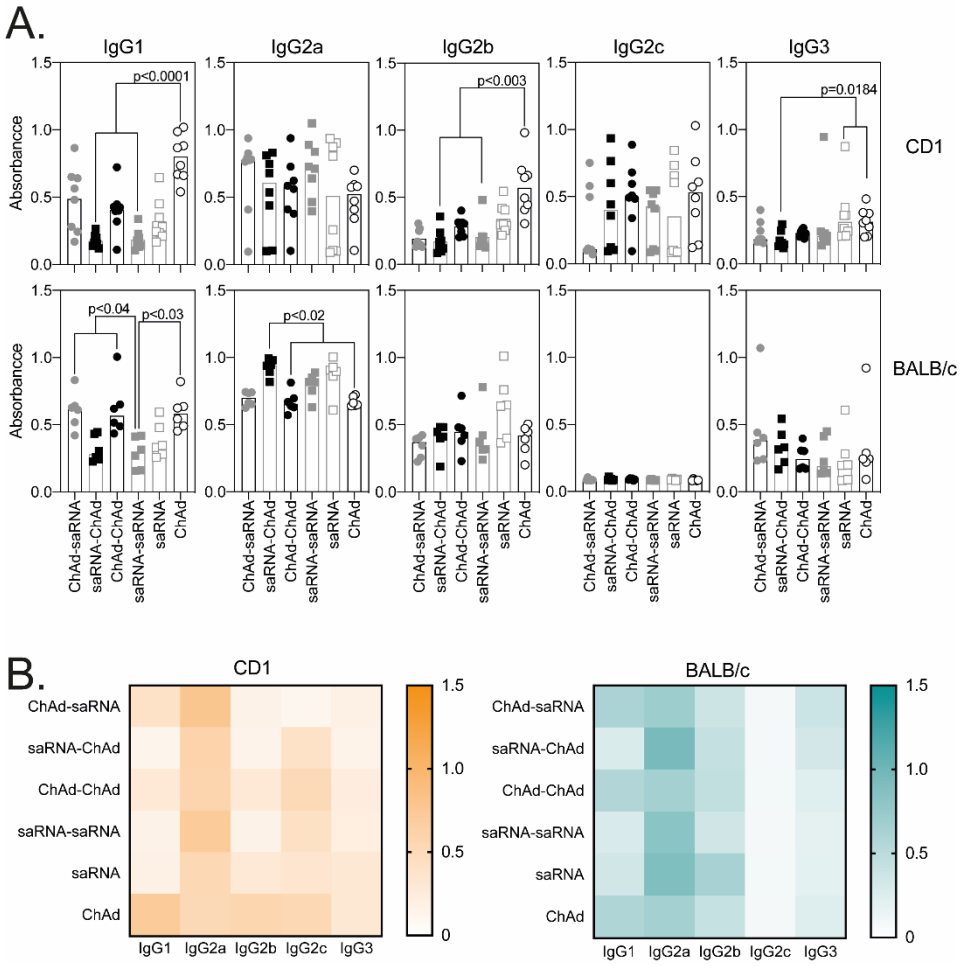

Fig 2: SARS-CoV-2 spike-specific IgG subclasses following ChAd and saRNA vaccination

For detection of IgG subclasses, each sample was diluted to 1 IgG ELISA Unit. Graphs show optical density measured against each IgG subclass where individual data points were expressed as an OD and shown here as scatter dot plots with bars showing the median (**A.**), followed by the heatmap summary representation with median response in each group to each IgG subclass (**B.**). Individual mice are represented by a single data point, bars represent the median response in each group (CD1 n=8; BALB/c n=6). Data in each graph was analysed with a Kruskal-Wallis and post-hoc positive test to compare differences between vaccination groups, p-values indicate significant differences between groups.

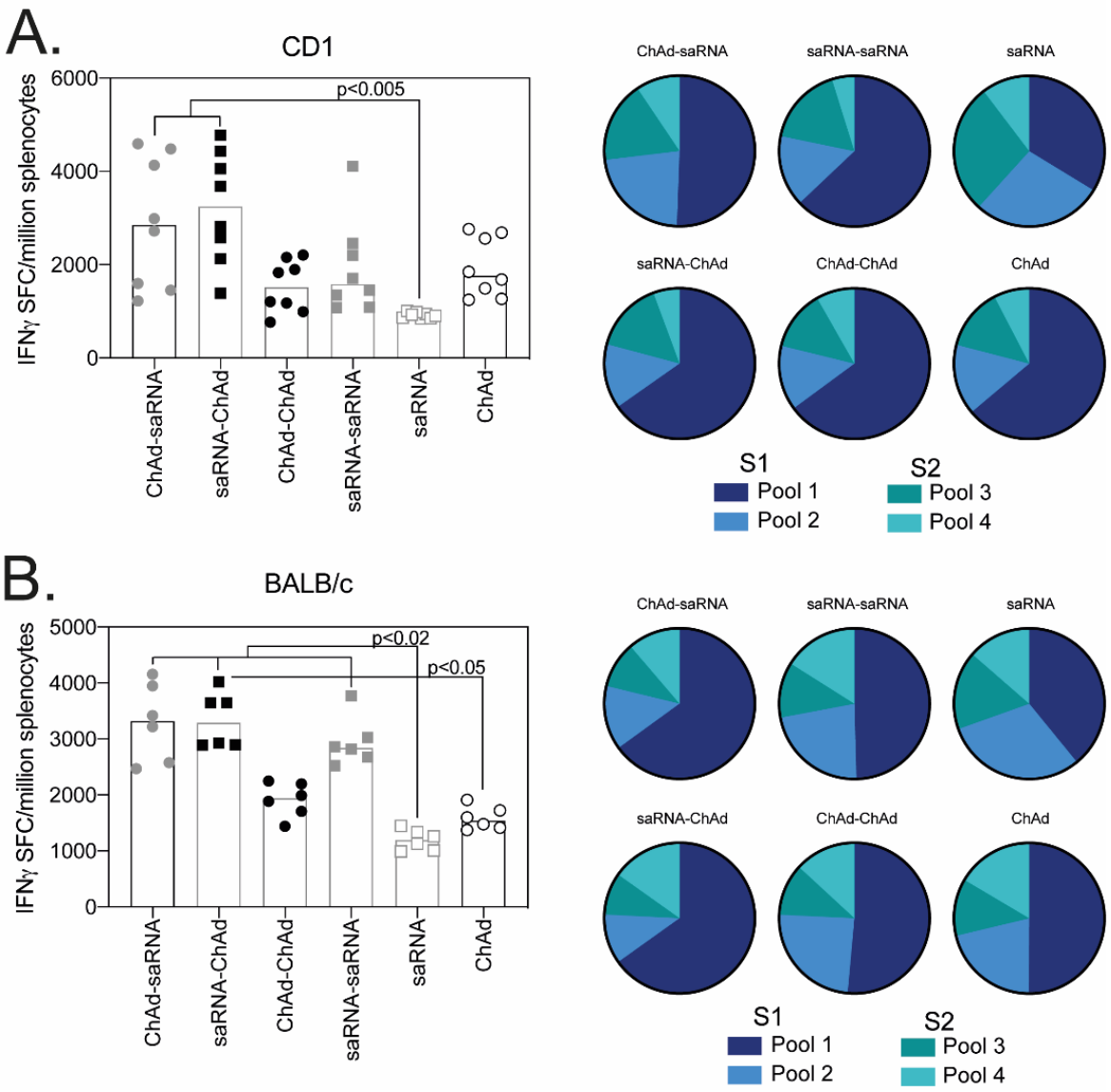

Fig 3: Breadth of T cell response measured by ELISpot

Graphs represent the total spike specific IFNγ response (sum of peptide pools) measured in outbred CD1 (**A.**) or inbred BALB/c (**B.**). Pie charts represent the response to each peptide pool as a proportion of total response. Data points represent individual mice and bars represent the median response in each group. Data in each graph was analysed with a Friedman test and post-hoc Dunn's multiple comparison to compare between vaccination regimens, p values are indicated on the graph.

423

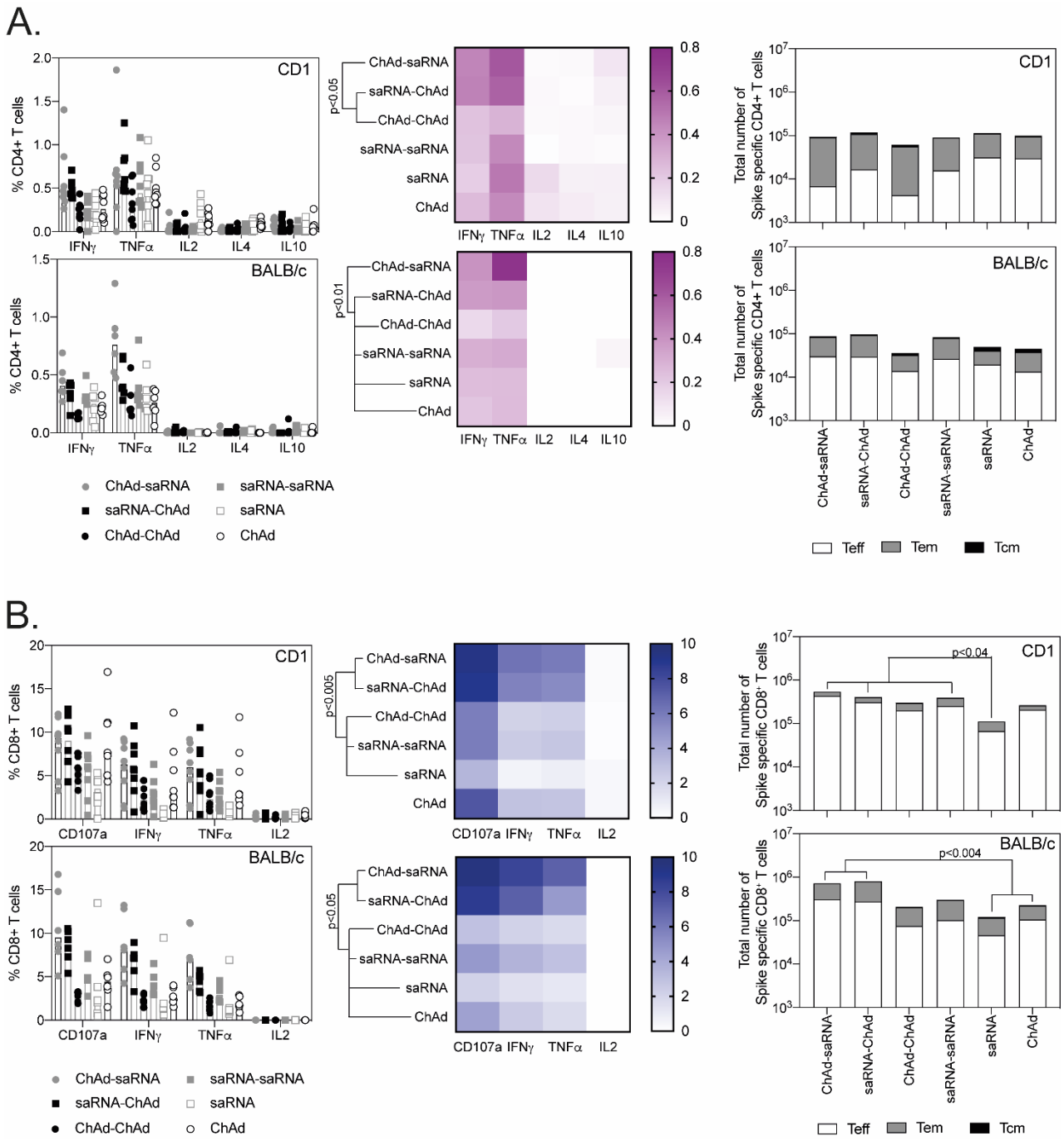

424

425 **Fig 4: Phenotype of the T cells response following vaccination**

426 Splenocytes were stimulated for 6 hours with pools of SARS-CoV-2 peptides prior to staining

427 for effector and memory T cells markers and intracellular cytokines. **A.**) Graphs show the

428 frequency of the spike-specific CD4^{+} T cells responses (left) in CD1 (top panel) and BALB/c

429 mice (bottom panel), heatmaps (middle) show the proportion of the response producing

430 each cytokine and total number of antigen specific cells of a T effector (Teff), T effector
431 memory (Tem) or T central memory (Tcm) phenotype (right). **B.**) Graphs show the
432 frequency of the spike-specific $CD8^+$ T cells responses (left) in CD1 (top panel; n=8) and
433 BALB/c mice (bottom panel; n=6), heatmaps (middle) show the proportion of the response
434 producing each cytokine and total number of antigen specific cells of a T effector (Teff), T
435 effector memory (Tem) or T central memory (Tcm) phenotype (right). Data points indicate
436 individual mice, bars represent the median response in each group. Total numbers of each
437 population are displayed in Fig S3C. Data in each graph was analysed with a two-way anova
438 and post-hoc Tukey's multiple comparison test to compare between vaccination regimens, p
439 values are indicated on the graph.
440
441
442

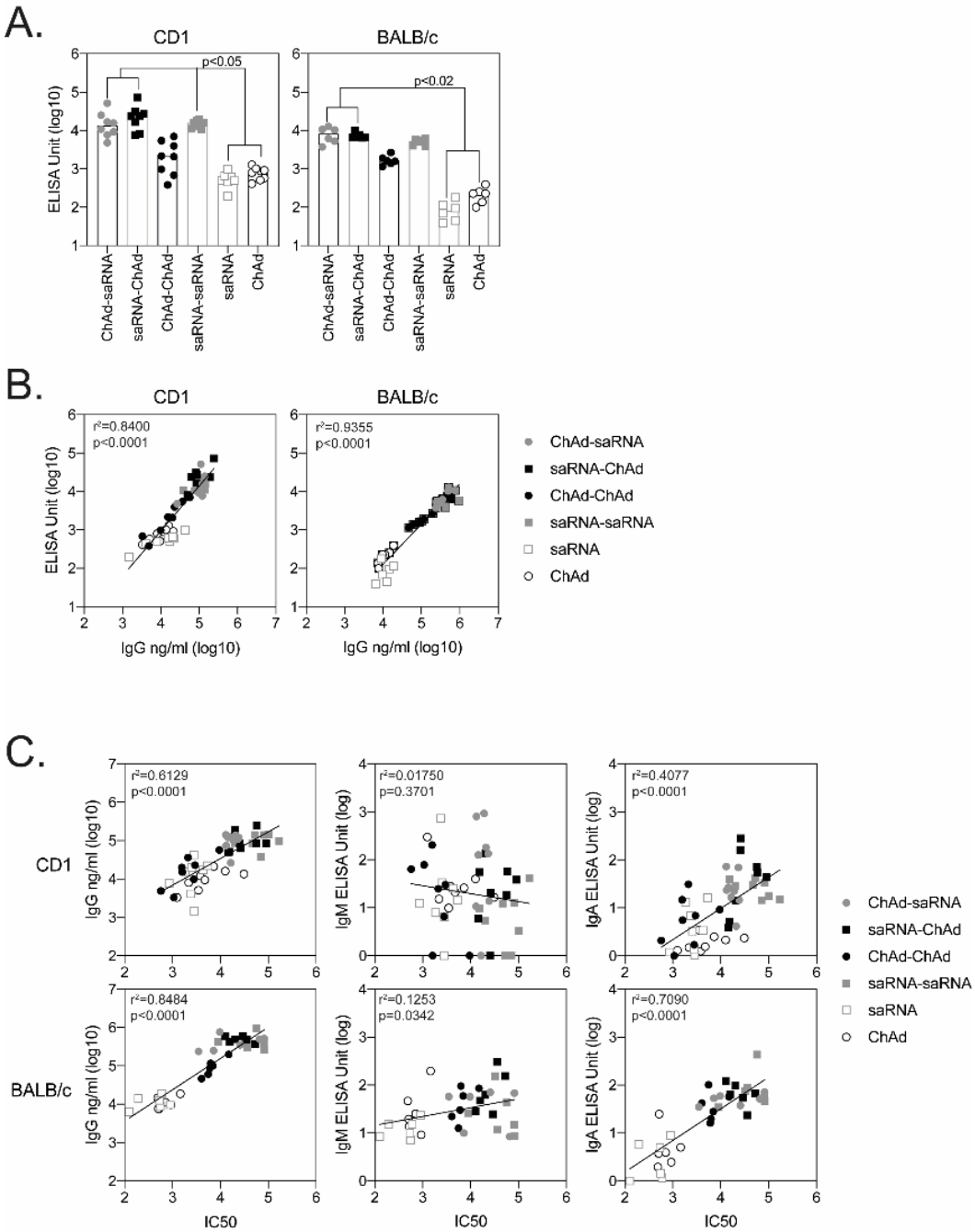

Fig S1: Comparison of assays measuring antibody responses after vaccination

SARS-CoV-2 spike-specific IgG responses were measured in a standardised ELISA (**A.**) and compared to IgG responses measured as a concentration (**B.**)

C.) Graphs show relationship between IgG, IgM and IgA responses to SARS-CoV-2 pseudoneutralisation IC50 values presented by linear

450 regression on log-transformed values. Data points represent individual animals from all

451 groups together, r^2 and p values are indicated on each graph.

452

453

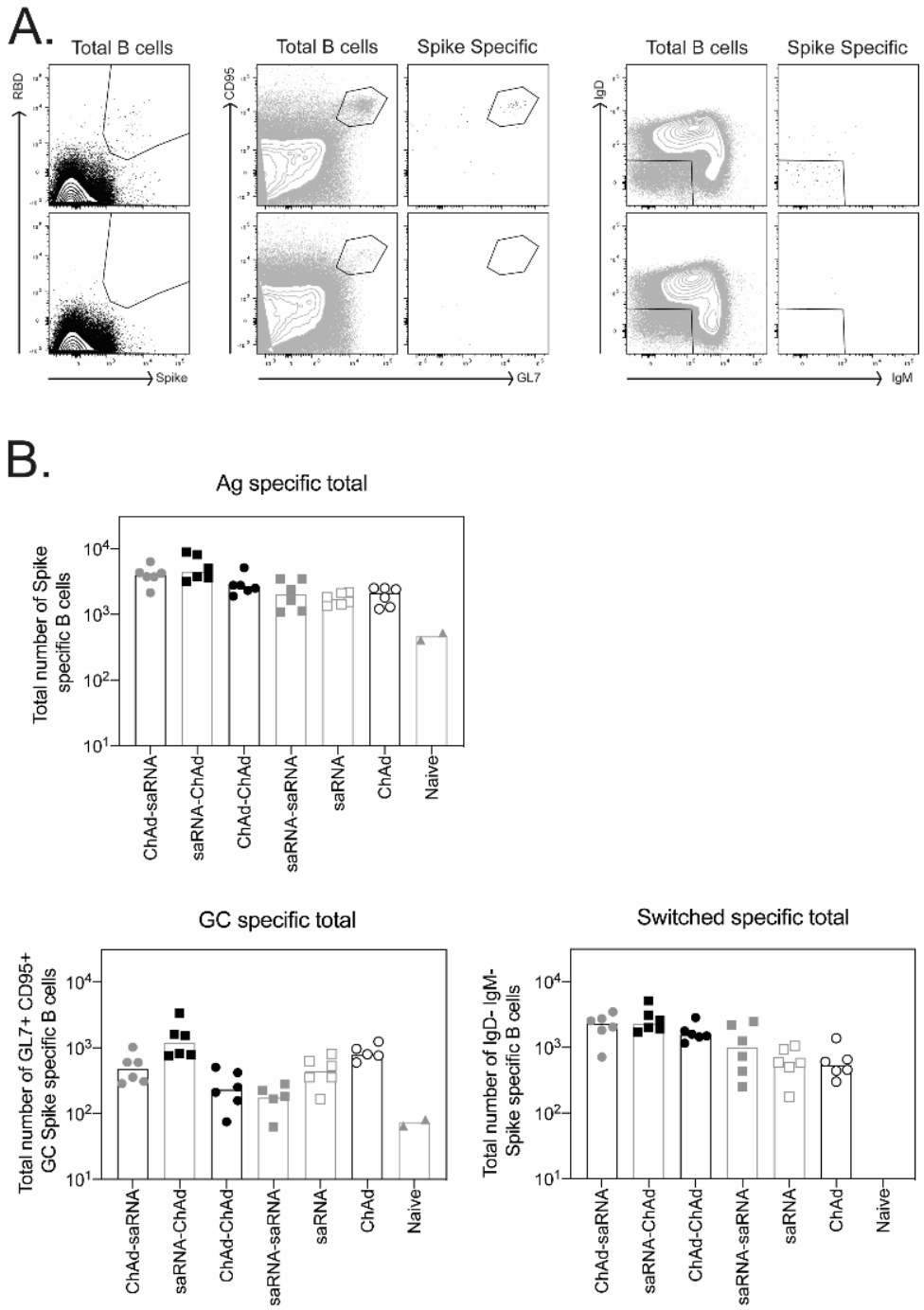

Fig S2: Antigen specific B cell responses

SARS-CoV-2 spike-specific B cells responses were measured in the spleen of BALB/c mice 3 weeks after the final immunisation. **A.**) Antigen specific cells were identified by staining with spike-PE and RBD-A647 tetramers. Germinal center (GC) B cells were identified as GL7+, CD95+, switched B cells identified as IgD- and IgM- antigen-specific B cells **B.**) Graphs show the total number of antigen-specific B cells, antigen-specific GC B cells and antigen-specific

461 switched B cells, data points are representative of individual mice, median responses per

462 group indicated by bars.

463

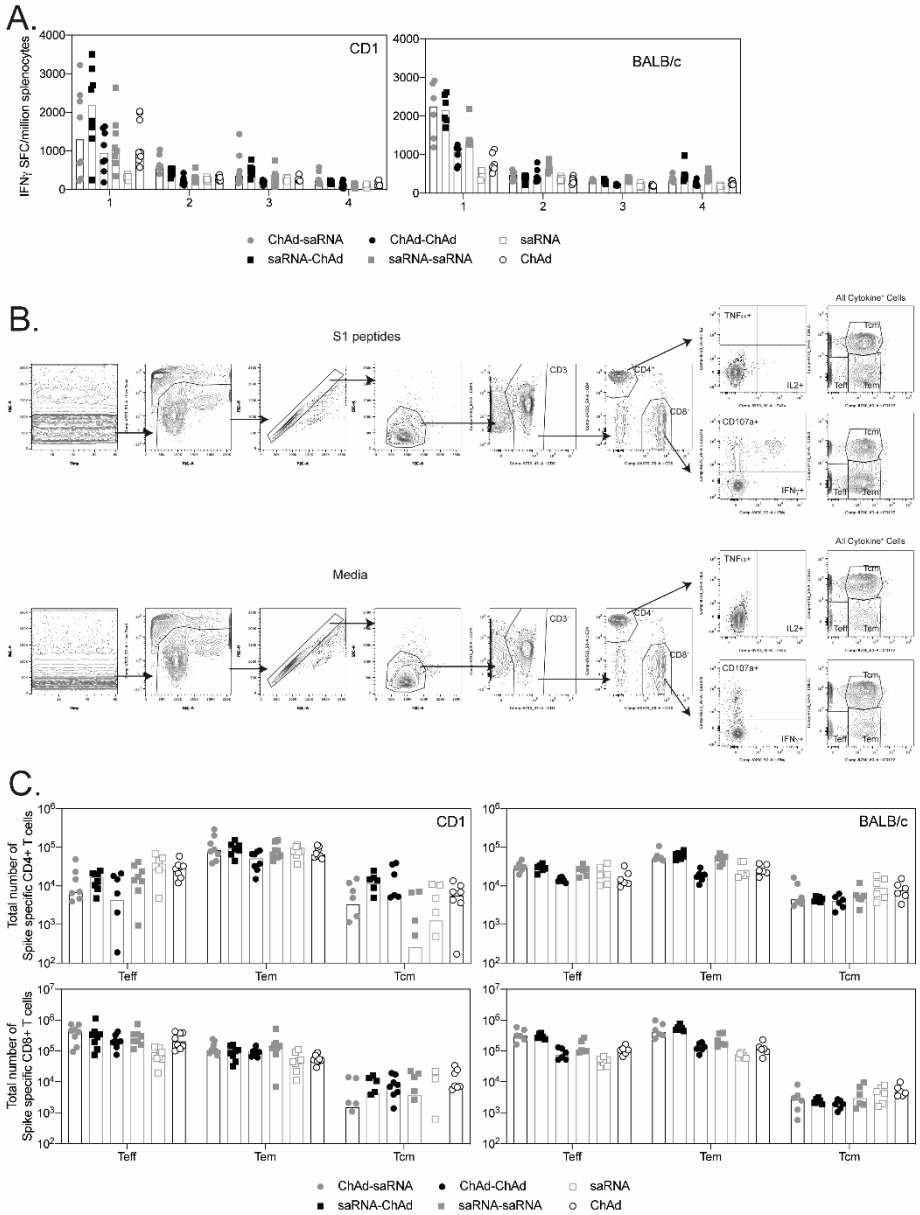

Fig S3: T cell responses measured by ELISpot and ICS

A.) Graphs show the IFNγ SFC detected to each pool of peptides by ELISpot. Each data point represents an individual mouse, bars represent the median response per group.

B.) Plots show the gating strategy used to identify antigen specific T cell responses.

C.) Graphs show the total number of Teff, Tem and Tcm responses detected in the spleens of mice. Each point indicates an individual mouse, bars represent the median response per group.